Aerosol Science and Technology 35: 637–647 (2001)

Published by Taylor and Francis
0278-6826/01/$12.00 + .00

Hygroscopic Properties of Pasadena, California Aerosol

David R. Cocker, III,[1] Nathan E. Whitlock,[2] Richard C. Flagan,[2] and John H. Seinfeld[2]

[1] *Department of Environmental Engineering Science, California Institute of Technology, Pasadena, California*

[2] *Department of Chemical Engineering, California Institute of Technology, Pasadena, California*

The hygroscopic behavior of Pasadena, CA aerosol was continuously measured from August 15 to September 15, 1999 using a tandem differential mobility analyzer. Two dry particle sizes were sampled, 50 nm and 150 nm in diameter; humidification of the dry aerosol was carried out at 89% relative humidity. Complex growth patterns were observed for both size modes, with aerosol distributions splitting from a single mode at times to more than 6 modes. Diurnal profiles for the observed multiple peaks were noted, with the greatest number of measurable growth modes being found during the late night and predawn hours for 50 nm particles. For 150 nm particles, more modes were present during the afternoon hours, with the humidified aerosol becoming bimodal during the late night/early morning hours. Growth factors, defined as the ratio of humidified particle diameter (at 89%) to dry diameter, were determined for modes with significant number concentrations. Average growth factors over the sampling period for the 2 particle sizes ranged from 1.0 to 1.6. Hygroscopic growth increased in the latter half of the sampling period when forest fires were present. In short, treating this complex urban aerosol as a combination of "less" and "more" hygroscopic fractions is an oversimplification.

INTRODUCTION

The response of atmospheric particles to changes in relative humidity (RH) is important in determining ambient particle size since water generally constitutes a substantial fraction of the atmospheric aerosol. This hygroscopic behavior is governed by the chemical composition of the aerosol. Since the detailed chemical composition of the atmospheric aerosol is rarely known, measurement of the hygroscopic behavior of the population allows one to infer indirectly important features indicative of the composition. Urban aerosols arise from a complex mix of anthropogenic and natural sources including marine layer salt, soot from combustion processes, primary and secondary organic products, and dust. During the late night and early morning, the existing air mass mixes with air that is marine influenced. During the day, primary aerosol is emitted from vehicles, as well as commercial and industrial sources. Secondary aerosol is also created by the oxidation of gas-phase hydrocarbons to produce semivolatile products.

Key studies of the hygroscopic behavior of atmospheric aerosols are summarized in Table 1. The most common approach utilizes the tandem differential mobility analyzer (TDMA), in which an aerosol, size classified in one differential mobility analyzer, is humidified and the resulting size distribution is measured in the second analyzer. Hygroscopic growth data have been traditionally reported in terms of a less hygroscopic and a more hygroscopic peak growth mode. The shift of one or more modes upon humidification is usually reported in terms of a growth factor (GF), which is the ratio of the mean diameter of the humidified particles to that of the dry particles, $GF = (D_P(RH))/(D_P(RH_{dry}))$. Typical RHs used for humidification range from 80 to 90%. Observed GFs in the less hygroscopic mode of urban aerosol range from 1.0 (no growth) to 1.4; for the more hygroscopic mode, GF ranges from 1.1 to 1.8 (McMurry and Stolzenburg 1989; Zhang et al. 1996; Busch et al. 1999; Ferron et al. 1999). For marine boundary layer aerosols, GFs range from 1.5 to 2.1 (Covert and Heintzenberg 1993; Berg et al. 1998; Massling et al. 1999).

The splitting of a dry aerosol upon humidification into 2 modes reflects the chemical composition of the particles. In a study of aged continental aerosol, Swietlicki et al. (1999) observed 2 modes, a less hygroscopic mode with a GF of 1.12 and a more hygroscopic mode with a GF between 1.44 and 1.65. They postulated that the hygroscopic growth could be attributed entirely to the inorganic content of the aerosol: sulfate, nitrate, and ammonium ions.

In laboratory studies of secondary organic aerosol formation by photochemical oxidation of monoterpenes, Virkkula

Received 22 November 1999; accepted 1 June 2000.

This work was supported by the U.S. Environmental Protection Agency Center on Airborne Organics. Special thanks to Kathalena Cocker and Markus Kalberer for assistance with the experiments and the processing of the data.

Address correspondence to John H. Seinfeld, Department of Chemical Engineering, California Institute of Technology, Pasadena, CA 91125. E-mail: seinfeld@caltech.edu

Table 1
Available data on hygroscopic aerosol growth

#	Type of aerosol	Location	Dates	Technique	Conditions	Findings	Reference	Notes
1	Urban	Claremont, CA	Jun–Sep 1987	TDMA & impactor	Measured hygroscopic growth of 50, 200, and 500 nm particles	Aerosol split into two modes, nonhygroscopic and hygroscopic Hygroscopic GF: 1.12 for 50 nm particles, 1.19 for 200 nm particles, 1.46 for 500 nm particles	McMurry and Stolzenburg (1989)	
2	Urban	Claremont, CA and Grand Canyon, AZ	1987 and 1990	TDMA & impactor	Measured hygroscopic growth of 50 to 500 nm particles	Claremont. "less hygroscopic" particles did not grow, "more hygroscopic" had growth factors from 1.15 at 50 nm to 1.6 at 500 nm Grand Canyon: "less hygroscopic" GFs ranged from 1 (no growth) to 1.4, "more hygroscopic" GFs were around 1.5	Zhang et al. (1993)	a
3	Urban	Minneapolis, MN	Summers, 1993–94	TDMA & impactor	Separated more hygroscopic and less hygroscopic modes and determined composition	Less hygroscopic: 55% chain agglomerates; 33% irregular shapes; <10% each spheres & flakes. More hygroscopic: liquid droplets that contained sulfur and sometimes carbon or ionic species (Na^+ or K^+)	McMurry et al. (1996)	
4	Urban	Lindenberg, Germany	Jul–Aug 1998	TDMA	Tested hygroscopic growth of 50–250 nm particles	Bimodal growth: less hygroscopic: GF ranges from 1.0 to 1.2; more hygroscopic: GF ranges from 1.3 to 1.8	Busch et al. (1999)	
5	Rural Semi-urban Urban	Germany	Winter, Summer, Fall 1998	TDMA	Tested hygroscopic growth of 50–250 nm particles	Bimodal growth: LH: GF = 1.03; MH: GF = 1.37 Bimodal growth: LH: GF = 1.03; MH: GF = 1.33 Bimodal growth: LH: GF = 1.00; MH: GF = 1.30	Ferron et al. (1999)	
6	Marine boundary layer–ACE 1	Remote Southern Hemisphere ocean	Nov–Dec 1995	FSSP	Measured particle sizes as a function of ambient RH	Changes in particle volume, effective radius, and optical scattering are strongly related to RH	Baumgardner and Clarke (1998)	b

7	Marine boundary layer–ACE 1	Remote Southern Hemisphere ocean	Oct–Dec 1995	TDMA	Measured particles with dry diameters of 35, 50, 75, and 150 nm in the MBL of Southern Ocean	Non-sea-salt sulfate (nss) GFs: 1.56–1.62, 1.59–1.66, and 1.63–1.78 for 35, 50, and 150 nm. Sea-salt particles: 2.12 and 2.14 for 50 and 150 nm	Berg et al. (1998)	c
8	Marine boundary layer and continental	Arctic–Norway	Mar–Apr 1989	TDMA	Measured hygroscopic growth of 110, 200, and 310 nm particles from 20 to 90% RH	Two modes: more hygroscopic, GF = 1.45; less hygroscopic showed very little growth (appeared only with continental aerosol). All aerosols tested showed some growth	Covert and Heintzenberg (1993)	
9	Marine and continental	Southern Atlantic and Indian Oceans	Jan–Apr 1999	TDMA	Tested hygroscopic growth of 50–250 nm particles	Marine: unimodal GF of 1.9; Continental: bimodal GF, MH = 1.8, LH = 1.4	Massling et al. (1999)	
10	Aged continental aerosol	Northern England	Mar–Apr 1995	TDMA & cascade impactors	Tested hygroscopic growth of particles between 35 and 265 nm	Less hygroscopic GFs: 1.11–1.15, increasing slightly with particle diameter. More hygroscopic GFs: 1.38–1.69 increasing with particle diameter	Swietlicki et al. (1999)	d
11	Rain forest	Amazon rain forest	Mar–Apr 1998	TDMA	Tested hygroscopic growth of 35–264 nm particles	Unimodal GFs from 1.2 to 1.4 when taken from a dry state to 90% RH	Zhou et al. (1999)	
12	Fog	Po Valley, Italy	Nov 1989	TDMA	Tested hygroscopic growth of particles between 30 and 200 nm during fog episodes	Two modes: more hygroscopic mode had a mean GF of 1.44 ± 0.14; less hygroscopic mode had a mean GF of 1.1 ± 0.07. GFs and LH fraction varied day to day, but no size dependence was seen	Svenningsson et al. (1992)	
13	Secondary organic aerosol	N/A	1998	TDMA	Tested hygroscopic growth of SOA from smog chamber experiments. Used limonene, α-pinene, and β-pinene with and without seed	No seed: GFs of about 1.1 were observed. Ammonium sulfate seed: GFs started at about 1.5 before reaction and diminished with time to $\sim$1.1. GFs did not vary much with size, but larger particles took longer to reach the final GF	Virkkula et al. (1999)	

(*Continued on next page*)

Table 1
Available data on hygroscopic aerosol growth *(Continued)*

#	Type of aerosol	Location	Dates	Technique	Conditions	Findings	Reference	Notes
14	Household primary aerosol	N/A	1996	TDMA	Measured hygroscopic growth of aerosols from deep frying oil, grilling sausages, and burning wood	Particles from wood smoke w/o flame were 92% soluble material and had GFs of 1.5–2.5, depending on initial particle diameter	Dua and Hopke (1996)	e
15	Household primary aerosol	N/A	1993	TDMA	Measured hygroscopic growth of aerosols from incense, cigarettes, natural gas, propane, and candles	Average GFs:1.36–1.85. For all types, GFs increased with increasing particle diameter. Tested room air as background: growth ratio was 1.75 at 50 nm	Li and Hopke (1993)	
16	Inorganic salt: NaCl and $(NH_4)_2SO_4$	N/A	1990	TDMA	Tested hygroscopic growth with organic layers on particles	Organic coating decreases hygroscopic growth, but nonuniform coatings cause large variations in GF	Hansson et al. (1990)	
17	Inorganic salt (NaCl)	N/A	1998	TDMA	Tested hygroscopic growth with organic layers on particles	Organic coating decreases hygroscopic growth, but large concentration required to achieve the effect observed in field experiments	Hansson et al. (1998)	
18	Sulfuric acid	N/A	1998	TDMA	Tested hygroscopic growth with and without organic layers	Organic layer on particles decreases hygroscopic growth of particles	Xiong et al. (1998)	

[a] At Grand Canyon, growth factors varied from day to day, but did not vary significantly with size.
[b] FSSP = forward scattering spectrometer probe.
[c] Particles with less hygroscopic growth only present during periods of anthropogenic influence.
[d] Fitting a model to the data, the hygroscopic growth could be adequately described assuming only inorganic species interact with water vapor.
[e] Particles from oil, sausages, and wood w/flame smokes did not grow, even though they were 8–46% soluble material.

et al. (1999) found growth factors of about 1.09. For experiments in which no seed aerosol was used, terpene oxidation products constituted the entire aerosol and the hygroscopic growth factor remained nearly constant throughout the reaction. When ammonium sulfate seed aerosol was used, the growth factor decreased continually with the time of reaction, starting from about 1.5, a value typical of ammonium sulfate ($(NH_4)_2SO_4$), and dropping to 1.1 at the end of the experiment. All particle sizes studied exhibited this trend, although the process took more time with larger particles. These chamber-generated aerosols did not exhibit the 2 modes of growth often characteristic of ambient aerosols because all the particles were generated from the same source. Several hygroscopic growth studies of mixtures of inorganic and organic aerosols (Hansson et al. 1990, 1998; Xiong et al. 1998) found that organic layers on inorganic particles decreased the hygroscopic growth factor of the aerosol.

Assuming the atmosphere contains only 2 types of aerosol may, however, be an oversimplification. The age of the aerosol, the composition and amount of organic coating, and the origin of the aerosol and its history are all expected to affect the hygroscopic nature of the particles. We report here nearly continuous measurement of the hygroscopic behavior of the Pasadena, CA aerosol from August 15 to September 15, 1999. For most of the study, 2 dry sizes were studied, 50 nm and 150 nm in diameter. We show the diurnal behavior of the observed growth factors for each particle size. During several days of the study, forest fires were burning in the adjacent mountains. Measured growth factors during that period appear to exhibit influence from the fire-generated particles. We first describe the experimental procedure, then present the measured hygroscopic growth data.

EXPERIMENTAL PROCEDURE

The hygroscopic behavior of the atmospheric aerosol was measured using a TDMA (Rader and McMurry 1986). The experimental system, illustrated in Figure 1, is similar to that employed by McMurry and Stolzenburg (1989) in previous studies of hygroscopic growth. Outdoor air was dried to a RH of $<10\%$. Using the model developed by Kreidenweis et al. (1987), the centerline residence time in the drying column was estimated to be at least 10 times greater than the time necessary to completely dry the particles, barring any hysteresis effects. Once dried, the aerosol passes through a charger (Aerosol Dynamics,

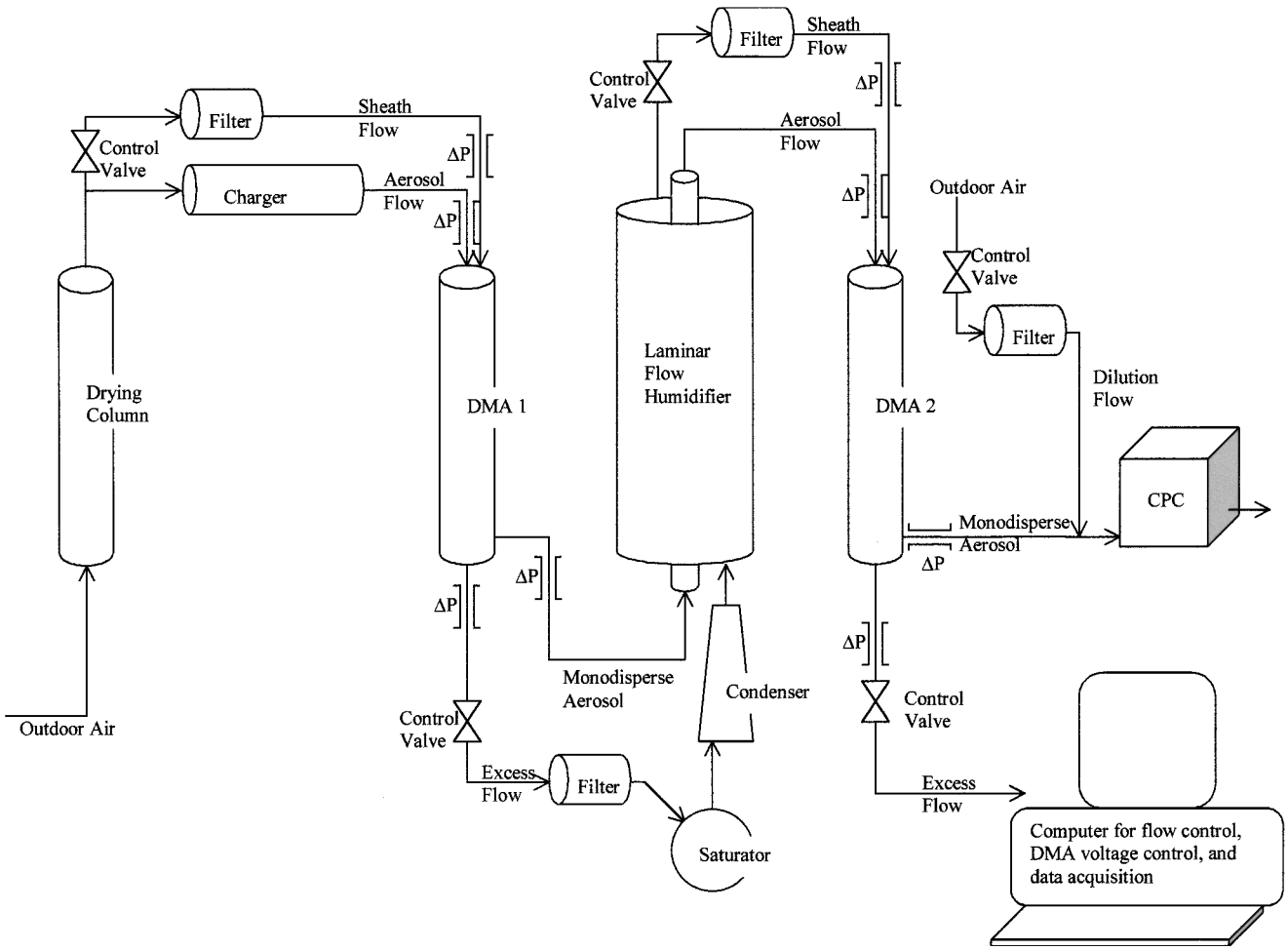

Figure 1. Experimental TDMA system.

Berkeley, CA) equipped with ^{210}Po strips to produce the steady-state Fuchs charge distribution (Fuchs 1963). The aerosol is then classified using a TSI Model 3071 differential mobility analyzer (DMA; TSI, Inc., St. Paul, MN) operated at constant negative voltage to produce a monodisperse aerosol.

The excess airflow from DMA1 is filtered and then humidified by passing it through a heated flask saturator containing distilled deionized water and finally through a condenser that is held at 0.1°C below room temperature. The classified aerosol and saturated air are introduced coaxially into a humidification tube 47 mm in diameter and 1003 mm long. A flow straightener is used to ensure laminar flow. The Reynolds number of the flow in this tube was 90, so the length required to achieve fully developed flow and a uniform distribution of water vapor is approximately 150 mm. With particles introduced at the center of the flow, variations in the residence time caused by the parabolic velocity profile are minimized. The RH in the tube is set at 89% by the ratio of dry to humid airflow rates. A water jacket around the humidification tube maintains its temperature.

The air exiting the humidifier enters a second DMA (DMA2) that operates as a scanning electrical mobility spectrometer (SEMS) with voltage scan times of 60 s. The flow from the outer annulus of the humidification tube is filtered before introduction into DMA2 as its sheath flow. The classified aerosol from DMA2 is mixed with filtered room air to produce the flow required for the TSI Model 3760 condensation particle counter (CPC) that is used to count the number of particles transmitted in 1 s time intervals. The particle size distribution is determined from particle counts after correction for the effects of multiple charging, diffusional broadening in the transfer function, and smearing due to the mixing effects within the CPC using the data inversion algorithm of Collins et al. (2001).

Precision TDMA measurements of particle growth require that all 4 flows entering and leaving each of the DMAs be accurately controlled. To achieve this degree of control continuously over weeks, all flow ratios were monitored by measuring pressure drops across calibrated capillaries using Dwyer (Michigan City, IN) Model 607-4 differential pressure transducers, interfaced to a personal computer with a National Instruments (Austin, TX) Model PC-LPM-16PnP data acquisition board that also records the number of particles from the CPC. A data acquisition and control program written in National Instruments LabView operates the 5 proportional flow control valves (Models 0248A-50000S V and 0248A-20000S V, MKS Instruments, Andover, MA) up to 100 times per second through an analog output card (Model PCI 6713, National Instruments). This control system maintains all of the flows at the desired levels without passing any aerosol through flow control valves.

The TDMA system sampled the Pasadena aerosol continuously from August 15 to September 15, 1999, with a gap from September 3–6. Prior to August 25, DMA1 was set to classify ambient particles at 50 nm diameter. Thereafter it alternated between 50 and 150 nm, with 3 consecutive scans at each size. A delay was added before the first scan at a size to ensure that a representative sample was being attained. The entire cycle (6 scans and 2 delays) required approximately 20 min. Additionally, an ozone detector (Model 1008-PC, Dasibi Environmental Corp., Glendale, CA) monitored ozone mixing ratios.

ANALYSIS OF 50 nm AND 150 nm PARTICLE DATA

The data obtained were analyzed as 2 distinct sets: "normal" Pasadena summer aerosol and fire-influenced Pasadena summer aerosol. No fires were present from August 15 to August 28. Most days, the high temperatures were 35–40°C. All days were clear by late morning after the marine layer burn-off. On August 29, a wildfire in the nearby San Gabriel Mountains broke out and was not contained until September 5. A major forest fire ignited in the San Bernardino Mountains (50 miles to the east) on August 29 and burned out of control until September 6, when it was contained. It was finally extinguished by September 15. On the days of August 30, August 31, and September 3, meteorological conditions were such that visibility decreased at the sampling site and a pervasive odor of smoke was present. For the entire period from August 29 to September 15 there were wildfires in other regions in the South Coast Air Basin, all within 50 miles of the sampling site in Pasadena. No TDMA data are available from noon September 3 until the morning of September 7 due to an operator error. A recurring computer error caused a number of small gaps in the data.

From August 15 to August 24, only the 50 nm aerosol (size exiting the first DMA) were sampled and analyzed. Starting on August 25, 150 nm and 50 nm sizes were sampled with 3 scans of each separated by a 3 min delay. The calibrated size of the 50 nm and 150 nm data were 49.7 nm and 148.5 nm, respectively. The accumulation mode aerosols investigated (50 nm or 150 nm) are produced via evaporation of larger particles, by combustion or by photochemical precursors. The aerosol is so fine that mechanical processes such as entrainment of mineral dust, construction artifacts, or tire or brake wear are unlikely to contribute significantly.

Virkkula et al. (1999) suggested that the hygroscopic growth of their smog chamber-generated aerosol could be separated into that attributed to organic and inorganic fractions. A seed aerosol composed of pure $(NH_4)_2SO_4$ was coated with the semivolatile organic products of the α-pinene/ozone reaction. The hygroscopic GF of the mixed chamber aerosol could then be estimated from the volume fraction of the organic(ε_o) and inorganic $(1 - \varepsilon_o)$ components:

$$GF = \sqrt[3]{\varepsilon_o GF_o^3 + (1 - \varepsilon_o) GF_i^3}, \quad [1]$$

where GF_o and GF_i are growth factors of the organic and inorganic fractions, respectively.

Ambient air is more complex than that in a controlled chamber experiment, containing a much larger number of inorganic and organic compounds. The "history" of the ambient aerosol is also much more varied. However, particles that contain more

organic compounds will generally exhibit lower GFs than the pure inorganic salts. Particles containing substantial amounts of black carbon should exhibit very little, if any, hygroscopic uptake of water.

The 50 nm and 150 nm aerosol particles do not necessarily exhibit similar hygroscopic properties since their organic–inorganic fractions may differ. A small organic layer on a 50 nm particle amounts to a significant organic volume fraction. Particles of 150 nm may have a significant inorganic fraction which corresponds to a more hygroscopic fraction.

Primary aerosol particles with diameters of 40–250 nm from anthropogenic sources typically contain a large fraction of organics. For example, Kleeman et al. (2000) found that the organic content of 40–250 nm diameter primary aerosol particles emitted by motor vehicles ranges from 85% to 95%. For wood smoke, aerosol in the 40–250 nm diameter size range, organic material constitutes between 65% and 95%, depending on the type of wood (Kleeman et al. 1999); charbroiling meat smoke and cigarette smoke were found to have an organic content of about 67% and 98%, respectively. Therefore primary aerosol released by these anthropogenic sources is expected to exhibit a relatively low GF.

Particles generated in the marine boundary layer are largely inorganic, composed primarily of sea-salt. These aerosols have measured water uptake factors of 1.5 to 2.1 Marine and anthropogenic aerosol should therefore be easily distinguished. However, atmospheric particles continuously change as semivolatile secondary organic compounds, derived from oxidation of hydrocarbons in the atmosphere, coat the preexisting sea-salt and anthropogenically derived aerosol. Both the time over which the particles may have been exposed to condensable vapors and the initial particle size influence the ultimate hygroscopic behavior of the aerosol.

For each 50 nm scan taken during the study, the number of discernible peaks was counted. Only peaks with an integrated number of >1 count cm^{-3} were considered relevant. The number of peaks versus the time of day is displayed in Figure 2. Figure 2a gives a diurnal profile; 2b a 1 week profile; and 2c the profile for the duration of the experiment. The solid line represents a 5-point binomial smoothing algorithm. Each data point represents a single scan. Variability in the number of peaks on small time scales (scan to scan) are a result of the inability to distinguish individual peaks from scan to scan even though they may be present. The number of peaks produced by the humidified 50 nm aerosol exhibits a clear pattern with time of day throughout the experiment, with the smallest number of peaks present in the early afternoon (between 12 and 2 pm) and the most peaks present in the early morning (2–4 am). The pattern was not altered by emissions from the forest fires in the latter half of the study.

During the period from August 17 to August 23, only 50 nm aerosol was monitored. Over 3,500 89% ± 1% humidity scans were obtained. Each scan was analyzed by first counting the number of peaks and then fitting the data to a multimodal log-

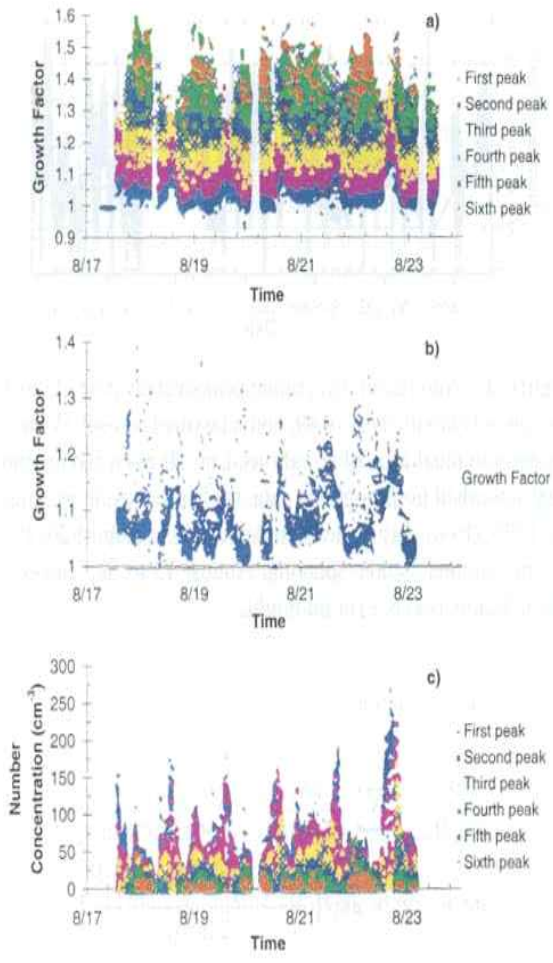

Figure 2. Number of discernible peaks versus time of day for the aerosol classified dry of 49.7 nm classified aerosol. Points indicate individual peak observations. Line shows a 5-point binomial smoothed fit through the data. (a) Diurnal cycle on August 19, 1999; (b) weekly cycle from August 18 to August 26, 1999; (c) the complete study, spanning August 13 to September 15, 1999. Tickmarks (b, c) at midnight.

normal size distribution, i.e.,

$$\frac{dN}{d\ln D_p} = \sum_i \frac{dN_i}{d\ln D_{p,i}} = \sum_i \frac{N_i}{(2\pi)^{1/2}\ln\sigma_{g,i}} \times \exp\left(-\frac{(\ln D_{p,i} - \ln \bar{D}_{pg,i})^2}{2\ln^2\sigma_{g,i}}\right), \quad [2]$$

by a least squares analysis. $\sigma_{g,i}$ is the standard deviation, $\bar{D}_{pg,i}$ is the mean aerosol diameter for the individual peak, $D_{p,i}$ is the diameter of each size bin, and N_i is the number of particles in the given peak.

Figure 3a displays the GFs for each of the log-normal distributions. Peak number 1 corresponds to the smallest diameter. Figure 3b shows the GF of the dominant peak, i.e., the one that contains the largest particle number concentration. Figure 3c shows the particle number concentration of each individually fit aerosol peak. Several trends are identifiable from careful consideration of these data. First, the locations of the first several peaks indicate that the hygroscopic GF of the aerosol does not vary much throughout the week for these modes. The first peak ranges from 1.0 to 1.1, the second from 1.04 to 1.2, and the third from 1.12 to 1.3. Only the last 3 peaks range more widely. Furthermore, most of the aerosol grows only slightly when exposed to high humidity. This suggests that the main fraction of the aerosol is composed of either organic material or soot, both of which have low hygroscopic GFs. The hygroscopicity of the main fraction (based on number concentration) increases during the afternoon. This is also consistent with a mostly organic aerosol. This "peak" in the hygroscopic GF in mid-afternoon corresponds to the peak in photochemical activity as measured by ozone concentration. This trend is consistent with chamber data, which shows an increase in the hygroscopic growth of organically coated aerosol as it becomes increasingly oxidized. The greater oxidation levels can lead to more acids and aldehydes, increasing the polar organic content and therefore its hygroscopicity.

Hygroscopic Behavior of 50 nm Particles

Figures 4a–i contain sample distributions taken from DMA2 for 50 nm diameter classified aerosol on August 26. These sample distributions are typical for the duration of the study. The timing of the monomodal distribution peak varies by 1–2 h. The hygroscopic growth of the 50 nm particles increased slightly during the fires, but the size distribution pattern remained constant. Figure 4a shows the calibrated aerosol distribution that was obtained by maintaining the same RH in the first and second DMA. Figures 4b–i show a sequence of humidified aerosol size distributions throughout the day and reveal a pattern. Several peaks merge during the morning, becoming unimodal about 2:30 pm. The aerosol then separates into multiple modes throughout the rest of the day, as might be expected if the secondary aerosol were primarily organics. The hygroscopic particles that form multiple peaks in the early morning may grow out of the 50 nm size

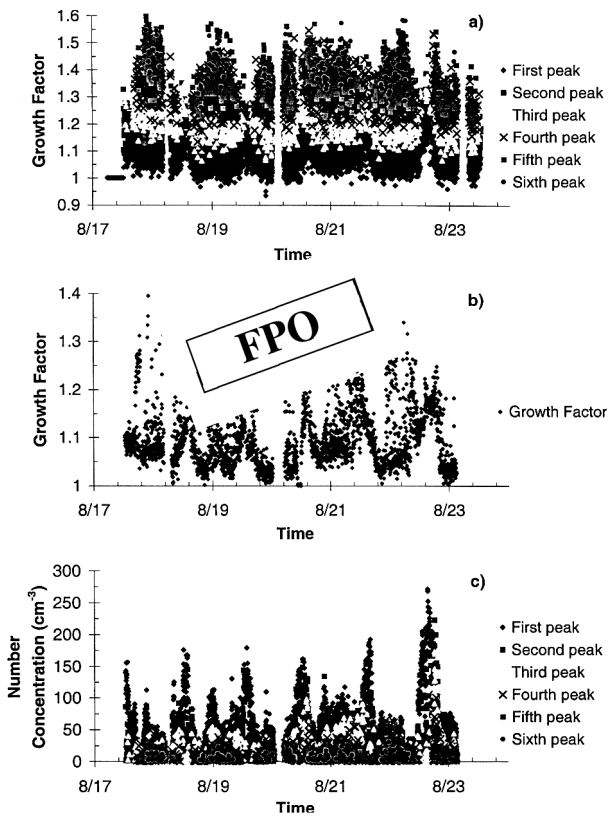

Figure 3. Measured GFs for log-normally fit peaks of 49.7 nm dry particles humidified to 89% RH for August 17 to August 23. (a) GF for each peak; (b) GF of the peak containing the greatest number percent of particles in the size distribution from DMA2; (c) particle number concentration of each individually fit aerosol peak. Major tickmarks at midnight.

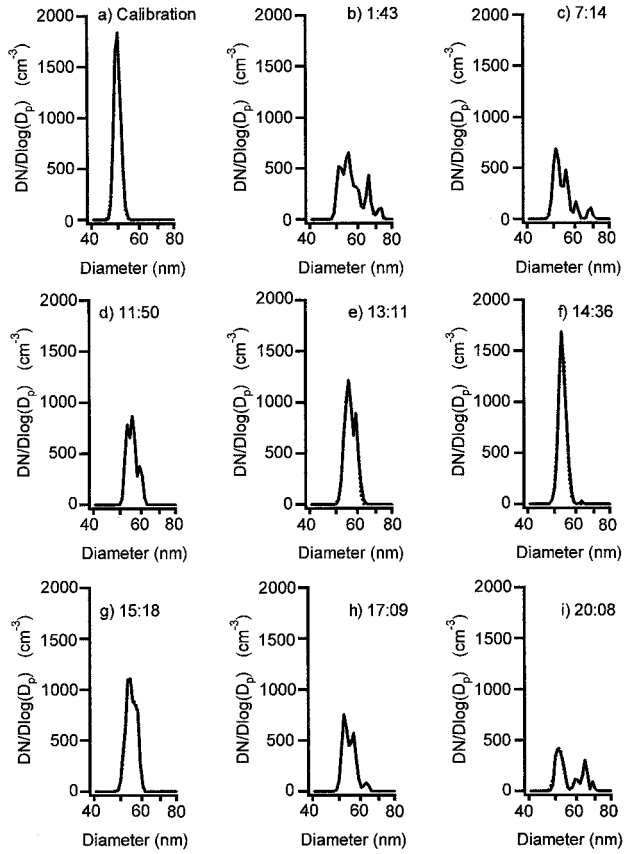

Figure 4. Typical size distributions from DMA1, classification set to 49.6 nm. The solid line shows experimental data; the dashed line shows a multimodal log-normal fit. (a) Distribution before humidification; (b–i) representative distributions on August 26, 1999.

range as they are coated by secondary organic products, or the coating process may reduce the hygroscopicity by producing an aerosol that is mostly organic. In the late afternoon and evening, transport of aerosol dominated by inorganic salts increases the hygroscopicity of the Pasadena aerosol. The appearance of multiple peaks suggests that a variety of sources contribute to this aerosol. During the night, marine aerosol can be transported to the site without undergoing any photochemical processes, as evidenced by the largest hygroscopic peaks appearing at night. Because the hygroscopic growth factors rarely reach 1.5, we may infer that few particles in the Pasadena aerosol are pure marine aerosols, even at night when the winds originate at the coast.

TDMA experiments performed on chamber aerosol at Caltech show that the $(NH_4)_2SO_4$ seed particles decrease in hygroscopic growth as they are coated with secondary organics. However, continued photochemical reactions after the primary hydrocarbon was reacted led to an increase in the hygroscopic growth. Similar transformations of aerosol-phase organics may occur in the ambient aerosol, contributing to the increase in hygroscopicity later in the day as seen in the data.

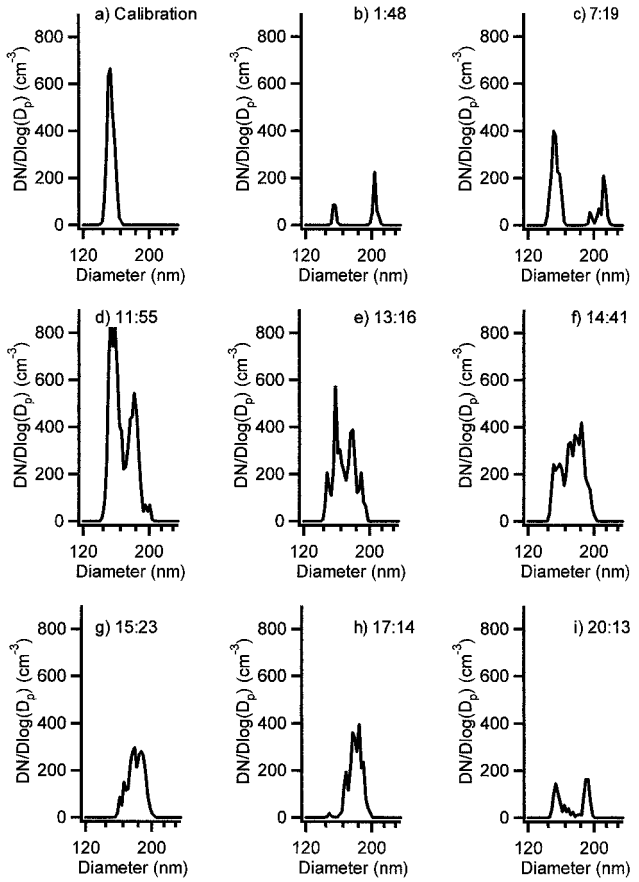

Figure 5. Typical size distributions from DMA1, classification set to 148.5 nm. (a) Distribution before humidification; (b–i) representative distributions on August 26, 1999.

Hygroscopic Behavior of 150 nm Particles

Figures 5a–i contain sample distributions taken from DMA2 for 150 nm classified aerosol on August 26. These sample distributions exhibit a pattern that is typical of that observed throughout the study. Figure 5a is the calibrated aerosol distributions obtained by maintaining identical RH on the aerosol entering the first and second DMAs. Figures 5b–i illustrate that the size distributions differ substantially from those of the 50 nm particles. Fewer peaks are observed in the middle of the night, while the greatest number appear during the day. In spite of the obvious differences, this behavior suggests that the aerosols undergo similar atmospheric transformations as the 50 nm particles. The differences can be attributed to differences in the relative amounts of organic and inorganic aerosol in the 2 size fractions. Much more organic coating is necessary for the 150 nm aerosol to go from mostly inorganic, if marine in origin, to mostly organic by volume. At 1 am, the distribution is clearly bimodal; 1 mode has a large GF of about 1.6 and the other mode is barely hygroscopic with a GF of 1.1. This is consistent with aerosol from two different sources, one a primary aerosol, probably anthropogenic in origin, while the other aerosol mode is most likely marine in origin and therefore mostly inorganic. During the day the splitting becomes more prevalent as the organic coats the aerosol leading to particles with lower inorganic fractions. However, because the particles start larger, the organic fraction is unable to dominate. A range of compositions or perhaps coating thicknesses cause the aerosol to separate into several modes.

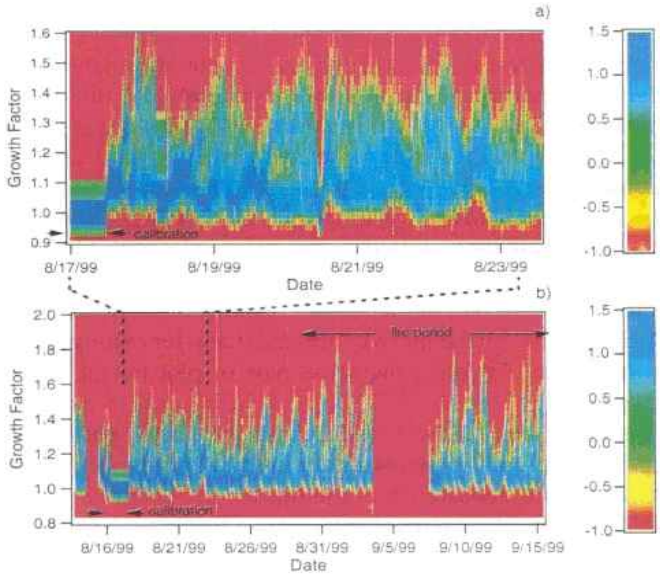

Figure 6. Cumulative distributions for the entire 49.7 nm classified aerosol, humidified to 89% RH. Color represents log of particle number concentration in each size bin. The period of fire influence is indicated. (a) Detailed data for the week of August 17 to August 23, 1999; (b) all data, August 13 to September 15, 1999. Tickmarks at midnight.

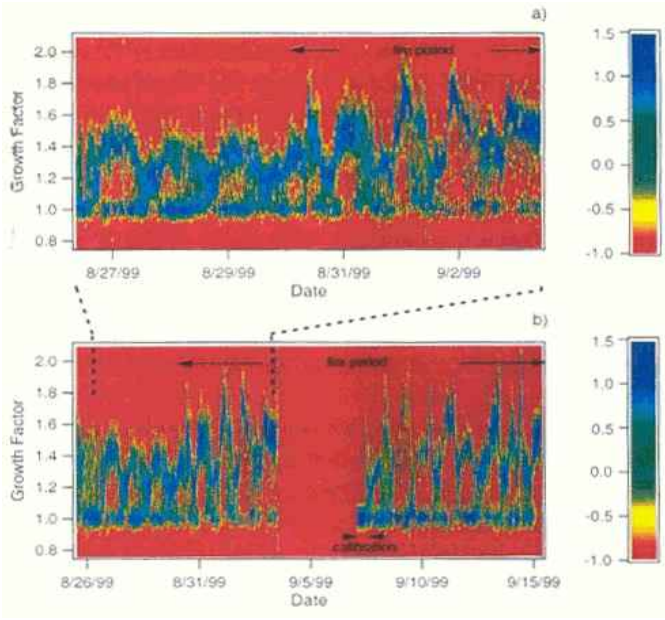

Figure 7. Cumulative distributions for the entire 148.5 nm classified aerosol, humidified to 89% RH. Color represents log of particle number concentration in each size bin. The period of fire influence is indicated. (a) Detailed data for the week of August 27 to September 3, 1999; (b) all data, August 26 to September 15, 1999. Tickmarks at midnight.

SUMMARY AND CONCLUSIONS

Figures 6a and 6b show a compilation of all the 50 nm scans over the entire period of measurement. Figure 6a shows a 1 week period to illustrate the diurnal cycle. Figure 6b shows the data for the entire experiment. The plots were generated by dividing the size distribution into 71 size bins where $\log(D_i/D_{i+1})$ (D_i and D_{i+1} represent classified aerosol diameters in bin i and $i+1$) is constant for all size bins. The total number concentration of particles in each size bin was computed. The log (% number) in each bin was then plotted as the color axis, with blue being the largest and red being <0.1% by number. The ordinate is the GF for each bin, defined as the log averaged diameter of each size bin divided by the mean calibrated diameter exiting DMA2. Figures 7a and 7b show the same type of plot for the 150 nm size aerosol.

Figures 6 and 7 indicate the duration of the fire periods. The hygroscopicity of the aerosol increased during the fire periods, but the general appearance of the diurnal cycle did not change. The 50 nm classified aerosol reduced to a single peak in the early afternoon, followed by a shift of the peak toward higher hygroscopic growth as the afternoon progressed. The 150 nm classified aerosol remained bimodal at night and multimodal during the day, which was also the observable trend without the fire.

The hygroscopic growth behavior of Pasadena, CA aerosol has been measured at 89% RH and reported. When humidified, both aerosol sizes, 50 nm and 150 nm in diameter, separated into multiple distinct modes depending on the time of day and size of the particles. Diurnal patterns were observed for the hygroscopic growth, with the largest modes present during the night and the lowest during the day. Differences in behavior of 50 nm and 150 nm particles were noted. The presence of wildfires in the vicinity of the sampling site led to an increase in aerosol hygroscopicity. In short, treating this complex urban aerosol as a combination of "less" and "more" hygroscopic fractions is an oversimplification.

REFERENCES

Baumgardner, D., and Clarke, A. (1998). Changes in Aerosol Properties with Relative Humidity in the Remote Southern Hemisphere Marine Boundary Layer, *J. Geophys. Res.* 103:16,525–16,534.

Berg, O. H., Swietlicki, E., and Krejci, R. (1998). Hygroscopic Growth of Aerosol Particles in the Marine Boundary Layer over the Pacific and Southern Oceans during the First Aerosol Characterization Experiment (ACE 1), *J. Geophys. Res.* 1013:16,535–16,545.

Busch, B., Sprengard-Eichel, C., Kandler, K., and Schutz, L. (1999). Hygroscopic Properties and Watersoluble Fraction of Atmospheric Particles in the Diameter Range from 50 nm to 3.0 μm during the Aerosol Characterization Experiment in Lindenberg 1998, *J. Aerosol Sci.* 30:S513–S514.

Collins, D. R., Flagan, R. C., and Seinfeld, J. H. (2001). Improved Inversion of Scanning DMA Data, *Aerosol Sci. Technol.*, in press.

Covert, D. S., and Heintzenberg, J. (1993). Size Distributions and Chemical Properties of Aerosol at Ny Alesund, Svalbard, *Atmos. Environ.* 27A:2989–2997.

Dua, S. K., and Hopke, P. K. (1996). Hygroscopic Growth of Assorted Indoor Aerosols, *Aerosol Sci. Technol.* 24:151–160.

Ferron, G. A., Karg, E., Busch, B., and Heyder, J. (1999). Hygroscopicity of Ambient Particles, *J. Aerosol Sci.* 30:S19–S20.

Fuchs, N. A. (1963). On the Stationary Charge Distribution on Aerosol Particles in a Bipolar Ionic Atmosphere, *Geofis. Pura. Appl.* 56:185–193.

Hansson, H.-C., Rood, M. J., and Covert, D. S. (1990). Experimental Determination of the Hygroscopic Properties of Organically Coated Aerosol Particles, *J. Aerosol Sci.* 21:S241–S244.

Hansson, H.-C., Wiedensohler, A., Koloutsou-Vakakis, S., Hameri, K., Orsini, D., and Widensohler, A. (1998). NaCl Aerosol Particle Hygroscopicity Dependence on Mixing with Organic Compounds, *J. Atmos. Chem.* 31:321–346.

Kleeman, M. J., Schauer, J. J., and Cass, G. R. (2000). Size and Composition Distribution of Fine Particulate Matter Emitted from Motor Vehicles, *Environ. Sci. Technol.* 34:1132–1142.

Kleeman, M. J., Schauer, J. J., and Cass, G. R. (1999). Size and Composition Distribution of Fine Particulate Matter Emitted from Wood Burning, Meat Charbroiling and Cigarettes, *Environ. Sci. Technol.* 33:3516–3523.

Kreidenweis, S. M., Flagan, R. C., and Seinfeld, J. H. (1987). Evaporation and Growth of Multicomponent Aerosols Laboratory Applications, *Aerosol Sci. Technol.* 6:1–14.

Li, W., and Hopke, P. K. (1993). Initial Size Distributions and Hygroscopicity of Indoor Combustion Aerosol Particles, *Aerosol Sci. Technol.* 19:305–316.

Massling, A., Wiedensohler, A., and Busch, B. (1999). Hygroscopic Growth of Aerosol Particles in the Southern Atlantic Ocean and Indian Ocean, *J. Aerosol. Sci.* 30:S837–S838.

McMurry, P. H., Litchy, M., Huang, P.-F., Cai, X., Turpin, B. J., Dick, W. D., and Hanson, A. (1996). Elemental Composition and Morphology of Individual Particles Separated by Size and Hygroscopicity with the TDMA, *Atmos. Environ.* 30:101–108.

McMurry, P. H., and Stolzenburg, M. R. (1989). On the Sensitivity of Particle Size to Relative Humidity for Los Angeles Aerosols, *Atmos. Environ.* 23:497–507.

Rader, D. J., and McMurry, P. H. (1986). Application of the Tandem Differential Mobility Analyzer to Studies of Droplet Growth or Evaporation, *J. Aerosol Sci.* 17:771–787.

Svenningsson, I. B., Hansson, H.-C., Wiedensohler, A., Ogren, J. A., Noone, K. J., and Hallberg, A. (1992). Hygroscopic Growth of Aerosol Particles in the Po Valley, *Tellus* 44B:556–569.

Swietlicki, E., Zhou, J., Berg, O. H., Martinsson, B. G., Frank, G., Cederfelt, S.-I., Dusek, U., Berner, A., Birmili, W., Wiedensohler, A., Yuskiewicz, B., and Bower, K. N. (1999). A Closure Study of Sub-Micrometer Aerosol Particle Hygroscopic Behaviour, *J. Atmospheric Res.* 50:205–240.

Virkkula, A., Dingenen, R. V., Raes, F., and Hjorth, J. (1999). Hygroscopic Properties of Aerosol Formed by Oxidation of Limonene, α-pinene, and β-pinene, *J. Geophys. Res.* 104:3569–3579.

Xiong, J. Q., Zhong, M., Fang, C., Chen, L. C., and Lippmann, M. (1998). Influence of Organic Films on the Hygroscopicity of Ultrafine Sulfuric Acid Aerosol, *Environ. Sci. Technol.* 32:3536–3541.

Zhang, X. Q., McMurry, P. H., Hering, S. V., and Casuccio, G. S. (1993). Mixing Characteristics and Water Content of Submicron Aerosols Measured in Los Angeles and at the Grand Canyon, *Atmos. Environ.* 27A:1593–1607.

Zhou, J., Swietlicki, E., Hansson, H. C., and Artaxo, P. (1999). Aerosol Particle Size Distributions and Hygroscopic Growth in the Amazonian Rain Forest, *J. Aerosol Sci.* 30:S163–S164.